

# Flow Driven Oscillating Vortex Generators for Control of Boundary Layer Separation

Todd R. Quackenbush<sup>1</sup>, Pavel V. Danilov<sup>2</sup>, and Glen R. Whitehouse<sup>3</sup>  
*Continuum Dynamics, Inc., Ewing, NJ, 08618*

Active flow control can be effective in tailoring boundary layer dynamics, but concepts developed to date have typically imposed significant design penalties because of the power and hardware required. This paper discusses the development and demonstration of a family of self-excited Flow Driven Oscillating Vortex Generators (FDOVGs) which oscillate at frequencies where the induced vortical flows have length scales that are of the order of the scale of the aerodynamic surface. FDOVGs receive power from the mean flow to operate and generate large amplitude oscillations that are useful for controlling boundary layer dynamics. This project entailed sequential concept development, analysis, design, fabrication, and testing of candidate FDOVG devices. Experimental activity included both studies of stand-alone FDOVGs as well as integrated tests of FDOVG arrays on lifting wings. Results clearly demonstrated the ability of these arrays to effect considerable improvements to attached flow with zero input power. In addition, several candidate mechanisms for deploying FDOVGs were developed, potentially enabling these improvements while also permitting device retraction, and, hence, yielding negligible cruise drag penalty. The demonstrations in hand are the first step in the development of micro- as well as macro-scale FDOVG devices with applications on micro air vehicles, UAVs, subsonic transports, and road vehicles.

## Nomenclature

$c$	= chord of VG surface
$h$	= device height
$\lambda$	= wavelength of longitudinal vortices
$F^+$	= reduced frequency
$x_{te}$	= distance from actuator to trailing edge
$U, U_\infty$	= free stream velocity
$U_{jet}$	= jet velocity
$\beta, \theta$	= angular displacements
$K_{a1}, K_{a2}, K_{f1}, K_{f2}$	= torsional spring rates
$C_{l\alpha}, C_{l\beta}$	= airfoil theory section lift curve slopes
$\gamma_1, \gamma_2$	= structural damping terms
$\rho$	= air density
$I_{xx}, I_{xy}, I_{yy}$	= FDOVG moments of inertia
$R$	= span of VG
$x_h$	= axial location of flap hinge from leading edge

## I. Overview

Recent work has involved the development and demonstration of Flow Driven Oscillating Vortex Generators (FDOVGs), a concept that offers many of the benefits of active separation control technologies without some of the key system integration penalties associated with alternative flow control systems. The central concepts behind FDOVGs (illustrated schematically in Fig. 1) are:

<sup>1</sup> Senior Associate, Continuum Dynamics, Inc., Senior Member AIAA.

<sup>2</sup> Associate, Continuum Dynamics, Inc., Member AIAA

<sup>3</sup> Associate, Continuum Dynamics, Inc., Senior Member AIAA

- The introduction of oscillatory longitudinal vortical structures that enhance mixing to postpone flow separation.
- Aeroelastic tailoring of the FDOVG to produce self-excited actuation at the required amplitude and frequency, eliminating the need for external mechanical actuators and power delivery requirements.
- Small size, minimizing cruise performance penalties for fixed installations.
- Optional deployment/retraction devices, eliminating cruise performance penalties with slightly higher installation cost and complexity.

The FDOVG devices are self-actuated through aeroelastic excitation by the flow stream eliminating the need for mechanical actuators. As part of this effort, several candidate configurations were designed that could introduce periodic streamwise vortex structures into the boundary layer flow region for separation control on representative lifting surfaces. A particularly successful variant was a flapped concept device that was fabricated and wind tunnel tested to demonstrate that a FDOVG can be designed which introduces large amplitude, long wavelength cyclic streamwise vortex structures into the flow.

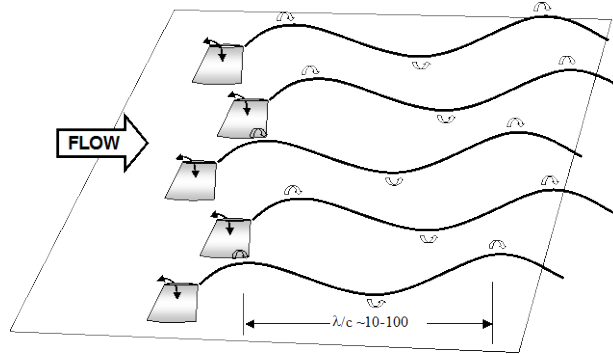


**Figure 1. Example array of flow driven oscillating vortex generators (FDOVGs). (note: here  $c$  is the mean chord length of the FDOVG surface and  $\lambda$  the wavelength of longitudinal vortices).**

The chief focus of this paper, however, is on a summary of the fabrication and testing of arrays of flapped FDOVGs as part of “capstone” wind tunnel tests. These test results not only demonstrated the functionality of the concept, but also illustrated its effectiveness as a flow control tool in

practical applications. One potential application is use of FDOVGs as cost-effective flow control devices for improved general aviation aircraft performance and safety. In addition, many new applications are anticipated once the geometric scalability demonstrated here can be appropriately exploited.

## II. Technical Background on Flow Control and Vortex Generators

It is well known that devices that introduce steady vortex structures or use steady blowing to energize boundary layers can postpone or even prevent flow separation. Classical fixed vortex generators (VGs) introduce longitudinal vorticity within or at the edge of the boundary layer, which in turn transfers high momentum fluid from the outer flow to the wall region to delay boundary layer separation. VGs consisting of a row of small plates or airfoils oriented normal to the surface and set at an angle of incidence to the local flow were first introduced by Taylor<sup>1</sup> and studied extensively in recent years by Lin<sup>2</sup>, among many others.

Over the last fifteen years great strides have been made beyond static VGs through the development of active control blowing concepts for control of boundary layer separation. Low Mach number and Reynolds number experiments have demonstrated that cyclic vortical oscillations introduced into a separating boundary layer slightly upstream of the average separation location can effectively delay boundary layer separation. This delay in boundary layer separation is directly related to enhanced mixing between the low momentum fluid near the wall and the external high momentum flow. For example, Seifert et al.<sup>3</sup> and later, Seifert and Pack<sup>4</sup> demonstrated that for single and two-element airfoils, oscillatory excitation becomes most efficient when the excitation frequencies correspond to the most unstable frequencies of the separating shear layer, generating arrays of spanwise vortices that are convected downstream. In these experiments the cyclic vortical oscillations were generated by oscillatory blowing through thin spanwise slots machined in the surface near either the airfoil leading edge or in the region of the flap knee.

In Ref. 3 it is shown that the most effective frequencies for increasing the lift are when the reduced frequency  $F^+$ , based on distance from actuator to trailing edge  $x_{te}$ , free stream velocity  $U_\infty$ , and excitation frequency  $f$ , is  $F^+ = fx_{te}/U_\infty \approx 1$ . Later in Ref. 4, similar oscillatory slot blowing performance was demonstrated for wings in low Mach number and aircraft scale Reynolds number conditions where optimal reduced frequencies were in the range of 0.5

to 1.5. This reduced frequency range result in one to three vortex structures over the controlled region at all times. These investigations demonstrated that small oscillatory excitation can have the same effect on delayed separation as steady blowing which is one to two orders of magnitude larger based on blowing momentum coefficient. Typically, unsteady momentum flux coefficients in the range of 0.3% were sufficient. The sensitivity of the flow to the reduced frequency was found to be small and it diminished with the introduction of steady blowing.

Similar delay in boundary layer separation has been demonstrated by McManus et al.<sup>5</sup> using pulsed vortex generator jets. With pulsed jets an array of jet orifices are positioned upstream of the potential separation region. The interaction between the jet and free stream flows gives rise to the formation of streamwise vorticity, which enhances mixing within the boundary layer, delaying boundary layer separation. Typically these jets are oriented at an angle relative to the free stream flow direction to enhance the generation of longitudinal vorticity. Under steady blowing conditions the vortical structures are very similar to conventional vortex generators. McManus et al.<sup>5</sup> have also shown that using unsteady pulsing of jets with velocity ratios  $U_{jet}/U_{\infty}$  as low as 2 can significantly delay separation (much below steady blowing requirements for the same delay), where  $U_{jet}$  is the maximum amplitude of the jet velocity.

A variation of the pulsed vortex generator jets is synthetic jets, which are actuated by small diaphragm driven cavities below the jet orifice<sup>6</sup>. Synthetic jets have the feature that there is zero net mass flux being introduced into the flow and therefore no need for supplied air or vacuum to drive the system. The cyclic flow structures introduced by synthetic jets are similar to pulsed jets, predominantly by the introduction of longitudinal vorticity<sup>7</sup>. One of the features of a jet issuing into a crossflow is the counter rotating vortex pair that is formed from the crossflow interaction. If the jet trajectory and the vortex pair remain confined into the boundary-layer region of the flow, then the jet/boundary-layer interaction has an effect similar to a passive vortex generator. The vortex pair transports high-momentum fluid at the edge of the boundary layer to the near-wall region, creating a fuller velocity profile that is better resistant to separation. The advantage of synthetic jets with respect to steady blowing or suction is that they need less momentum by one or two orders of magnitude to achieve equivalent effects. They also do not require a complex plumbing system because the momentum expulsion is only caused by the periodic motion of a diaphragm<sup>8</sup>. While zero net flux devices have been demonstrated for low speed and low Reynolds number applications, increasing the momentum flux (momentum coefficients) necessary for effective flow control on full scale aircraft in transonic flow poses a considerable challenge, as well as surmounting substantial installation problems. Current state-of-the-art zero net mass flux devices lack sufficient control authority and need effective coupling to most unstable flow modes<sup>9</sup>.

Research to date on these systems has clearly demonstrated that large delays in separation are possible with the introduction of very modest levels of oscillatory vorticity (either longitudinal or transverse vorticity). Furthermore, this research helped to identify the magnitude and frequencies of oscillatory vorticity that offer high levels of separation mitigation. Given the implementation challenges of these concepts, however, it would be highly desirable to develop a self-actuated device that harnesses the tremendous energy available in the free stream under normal operating conditions. The FDOVG concept was developed to fill this need.

### III. The Flow Driven Oscillating Vortex Generator (FDOVG) Concept

In initial work on this concept, a mechanism was sought that could introduce cyclic vortical structures that is simple, requires minimal power, does not require major redesign of the target application to integrate; an additional goal was to identify a device that has minimal impact on the system performance when not in use. In surveying current active control technologies it was noted that there are many ways to generate longitudinal cyclic vortical structures, with one of the simplest being active oscillation of a vortex generator. A schematic of such a device is presented in Fig. 2. As shown in the figure, a vortex generator is driven through a cyclic motion resulting in unsteady

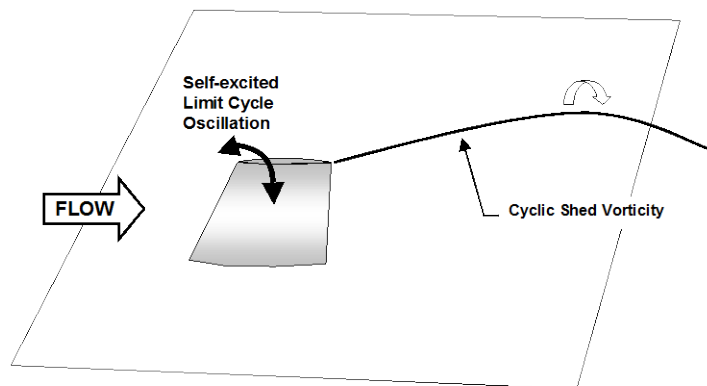


Figure 2. Flow Driven Oscillating Vortex Generator (FDOVG).

shedding of streamwise vorticity into the boundary layer region.

At first it would appear that this device could be actuated with a conventional mechanical or electric actuator. However, one needs only to examine the frequencies required to see that this will be very difficult. If the device is to be used during landing (where the characteristic free stream velocity is  $U \sim 150$  ft/s) or in front of a weapons bay, ( $U \sim 1000$  ft/s), assuming a vortex wave length of 5 ft. then the required actuation frequency is very high of order 30-200 Hz. Developing an actuator that would provide on the order of  $\pm 5^\circ$  of rotation at these frequencies would be a severe design challenge, given the high energy input required.

This challenge can be met, however, if it is possible to find a means to directly harness the energy in the mean flow. The key to this problem is the observation that an airfoil, which in this case is a vortex generator, can be aeroelastically tailored to undergo limit cycle oscillations (flutter) of a prescribed frequency and amplitude when exposed to a free stream flow as shown in Fig. 2. This is the Flow Driven Oscillating Vortex Generator (FDOVG) concept. Under such conditions the oscillatory motion is a self-excited motion with the power required to maintain the motion being extracted from the surrounding flow (passive actuation).

It is important to note that the length scale of the desired unsteady vortical flow structure is very different from that produced in a classical flutter problem. In the classical flutter problem the reduced frequency is order one and the wavelength of the shed vortical structure would be on the order of the VG chord. Further, since in general engineers design to avoid flutter, when limit cycle oscillation (LCO) does occur the amplitude of motion tends to be very small. To implement the FDOVG concept we are interested in introducing cyclic vortical structures that are on the order of ten to one hundred times the VG chord. For example, for separation control on a wing the length scale would be on the order of the wing chord, i.e.  $O(10-100)$  times the VG chord. Further, our objective is to introduce moderate amplitude vortical structures, which implies moderate amplitude VG motions. Therefore, a key element of the innovation in the FDOVG concept is designing a dynamic system that undergoes low frequency, moderate amplitude LCO motions. Moreover, these FDOVGs must be designed to meet multiple requirements for practical implementation as well as to demonstrate effectiveness in their aerodynamic flow control role.

#### **IV. FDOVG Design Process**

This section provides an overview of the concept development process for the FDOVG, including assembly of computational models that supported construction of bench top and wind tunnel test articles. This portion of the effort centered on a combination of prototyping and testing, derived from system specifications and requirements that were developed during meetings with potential end-users. This was followed by a conceptual design phase, which refined the feasibility demonstrator developed in earlier work and entailed a number of overlapping steps including: dynamic simulation modeling; spring/hinge mechanism development; concepts trades and prototyping; and preliminary design selection. This stage also featured assessment of alternative configurations (e.g., horizontal FDOVG concepts) and early studies of candidate deployment mechanisms. Following this early design stage, an iterative process ensued of quantification of FDOVG performance and effectiveness (via wind tunnel testing) and further cycles of detail prototype design and fabrication. This activity included fabrication of various scales of test devices as well as initial fatigue testing. Device design was directed at identifying concepts for the wind tunnel testing narrated in the next section.

##### **A. Identification of Potential FDOVG Mechanical Devices**

It has long been known that under certain conditions (generally to be avoided) wings and other dynamic systems will undergo limit cycle oscillation (LCO). Under such conditions, the energy required to maintain the LCO motion is being extracted from the surrounding flow field. For wing dynamics systems this is a special form of flutter where the energy extracted from the flow field is exactly equal to energy lost to structural, aerodynamic, and other forms of damping. There has been a great deal of research over the years developing methods for accurate prediction of the onset of LCO and flutter. In classical research on flutter the goal has been to predict flutter onset and then redesign the system to avoid any possibility of entering such conditions.

Regarding FDOVG device development, the goal of the present work was to develop a low aspect ratio vortex generator device which is designed to undergo a natural limit cycle oscillation at a prescribed flow speed and oscillatory amplitude and frequency. In this case the LCO phenomenon is used as a self-actuated mechanism for driving low aspect ratio vortex generators. Under such conditions the power required to maintain the motion is extracted from the surrounding flow and the oscillatory motion will result in cyclic shedding of longitudinal vorticity. Through aeroelastic tuning of the FDOVG structure it can be designed to oscillate (LCO motion) at a specified frequency and speed.

The amplitude and frequency characteristics of the FDOVG LCO phenomena can be tailored through the number of system degrees of freedom, choice of section properties, and combinations of construction materials and variation of root attachment mechanisms. Since for desired fatigue life there are limits to the range of motion which can be derived through structural deformation alone, particular attention has been directed toward the development of hinged or pinned attachment mechanisms which incorporate nonlinear springs. This approach provides a means of obtaining large amplitude LCO motions with minimal structural deformations.

In the opening phases of this project, a list of conceptual configurations was assembled upon which the proposed oscillating vortex generator could be based. The key in this initial study was to propose mechanisms that would introduce a natural oscillation into a vortex generator design to promote the unsteady shedding of streamwise vorticity. The particular goal was to identify configurations with the potential for generation of long wavelength periodic vortex structures,  $\lambda/c \sim O(10-100)$ , where  $\lambda$  is the wavelength of the vortex structure and  $c$  is the VG chord.

The most promising FDOVG concept was a flapped VG configuration shown in Fig. 3. This configuration incorporates a non-linear spring/hinge mechanism allowing pure bending motion at the VG root attachment point and a second spring/hinge mechanism at the flap attachment position. This concept is a two-degree of freedom system with pure bending motion of both hinges. The incorporation of hinges allows large amplitude motion without the requirement of large structural deformations. With careful design of the non-linear spring/hinge mechanisms and the mass distribution of the VG elements this system can be designed to undergo LCO motion at a prescribed amplitude and frequency. One of the main advantages of this concept is that each hinge is a single degree of freedom mechanism that is much easier to design.

## B. Dynamic Model Development

The first step in the development of this FDOVG concept was the formulation of a simple two-degree of freedom system dynamic model to determine the important scaling parameters in this configuration. This model was then used to guide in the design of a FDOVG configuration for demonstration of concept feasibility. As shown in Fig. 4, the flapped FDOVG concept is composed of a main airfoil section and a flap section. The main section is mounted to a fixed surface with a hinge located at  $y=0$  and allowing rotation  $\theta$  about the  $x$ -axis. This hinge

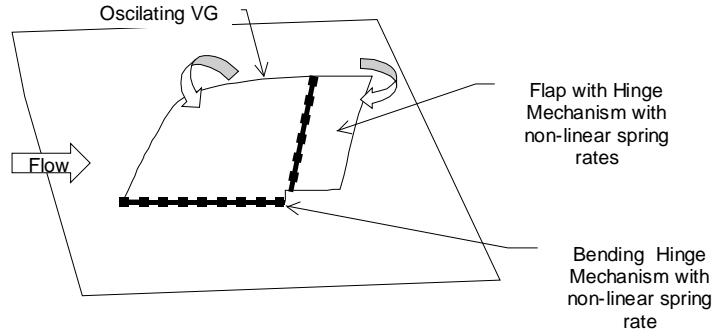


**Figure 3. Flapped oscillating VG concept using non-linear hinges.**

incorporates two torsional springs with rates  $K_{a1}$  and a non-linear spring rate  $K_{a2}$ , respectively. The flap is mounted to the main airfoil section with a second hinge located at  $x=0$  and allowing rotation  $\beta$  about the  $y$ -axis. This flap hinge also incorporates two torsional springs of rates  $K_{f1}$  and a non-linear spring rate  $K_{f2}$ .

Both non-linear spring rates are assumed to have the functional form shown in Fig. 5 with angular displacement  $\theta$  and  $\beta$ , respectively. As shown, the springs have characteristic angular displacement scales,  $\theta_s$  and  $\beta_s$ . For spring deflections less than  $\theta_s$  (or  $\beta_s$ ) there is zero spring moment for the non-linear spring component. The nonlinear spring component moments are given by:

$$\begin{cases} M_s = K_{a2}(\theta - \theta_s) & \text{for } \theta > \theta_s \\ M_s = 0 & \text{for } -\theta_s < \theta < \theta_s \\ M_s = K_{a2}(\theta + \theta_s) & \text{for } \theta < -\theta_s \end{cases} \quad \text{and} \quad \begin{cases} M_s = K_{f2}(\beta - \beta_s) & \text{for } \beta > \beta_s \\ M_s = 0 & \text{for } -\beta_s < \beta < \beta_s \\ M_s = K_{f2}(\beta + \beta_s) & \text{for } \beta < -\beta_s \end{cases}$$

Assuming rigid body dynamics for both the main airfoil and flap sections (of the FDOVG), this dynamic system can be modeled by the following set of coupled equations.

$$I_{xx}\ddot{\theta} - I_{xy}\ddot{\beta} + \left[ \frac{1}{6}\rho U^2 R^3 C_{l\alpha} + I_{xx}\gamma_1 \right] \dot{\theta} - I_{xy}\gamma_2 \dot{\beta} + [K_{a1} + K_{a2}g(\theta, \theta_s)]\theta - \frac{1}{4}\rho U^2 c R^2 C_{l\beta}\beta = 0 \quad (1)$$

$$\begin{aligned}
I_{yy}\ddot{\beta} - I_{xy}\ddot{\theta} + I_{yy}\gamma_2\dot{\beta} + \left[ \frac{1}{4}\rho U^2 c R^2 (C_{mf\alpha} + \frac{x_H}{c} C_{lf\alpha}) - I_{xy}\gamma_1 \right] \dot{\theta} \\
+ \left[ K_{f1} + K_{f2}g(\beta, \beta_s) - \frac{1}{2}\rho U^2 c^2 R (C_{mf\beta} + \frac{x_H}{c} C_{lf\beta}) \right] \beta = 0
\end{aligned} \tag{2}$$

where function  $g(x,y)$  is defined by:

$$\begin{aligned}
g(x,y) &= \frac{|x|-y}{|x|}, \quad \text{if } |x| > y \\
g(x,y) &= 0, \quad \text{if } |x| < y
\end{aligned} \tag{3}$$

The FDOVG aerodynamics is modeled assuming quasi-steady flow and thin airfoil theory.  $C_{l\alpha}$  and  $C_{l\beta}$  are thin airfoil theory section lift curve slopes as a function of angle of attack,  $\alpha$  and flap deflection angle,  $\beta$ , respectively. ( $C_{lf\alpha}$ ,  $C_{mf\alpha}$ ) and ( $C_{lf\beta}$ ,  $C_{mf\beta}$ ) are thin airfoil theory flap element lift curve and moment curve slopes as a function of angle of attack,  $\alpha$  and flap deflection angle,  $\beta$ , respectively. A simple finite wing aspect ratio correction was also incorporated into these coefficients. A first approximation to the structural damping was incorporated into this model for analysis of “living hinge” designs using an equivalent viscous damping term with coefficients  $\gamma_1$  and  $\gamma_2$ , corresponding to  $\theta$ - and  $\beta$ -motion structural damping, respectively.

A computer program was written to solve the coupled set of equations given above. The model was given a small initial angular velocity for both the root hinge and the flap hinge. The equations were then evolved in time until a periodic steady state solution was obtained or the solution damped to some equilibrium position. This computer simulation was found to be very helpful in both designing a suitable wind tunnel model test configuration to demonstrate concept feasibility, and also providing insight into the role that various system variables play in determining the overall system dynamics.

Using this dynamic simulation model a nominal 3” chord and 3” span flapped FDOVG configuration was designed that would demonstrate sustained oscillation in a 1’x 1’ wind tunnel. Since the maximum speed of this small wind tunnel is roughly 150 ft/s, the demonstration model was designed to undergo self-excited LCO below this maximum tunnel speed. Another important design consideration was to demonstrate that oscillatory vortical structures can be introduced having a wavelength much larger than the FDOVG chord (recall that  $\lambda/c \sim O(1)$  for classical flutter phenomena). To demonstrate feasibility of the concept the target here was in the range of  $\lambda/c \sim O(10-100)$ . Finally, to simplify model fabrication, the model was machined from 3/16 inch

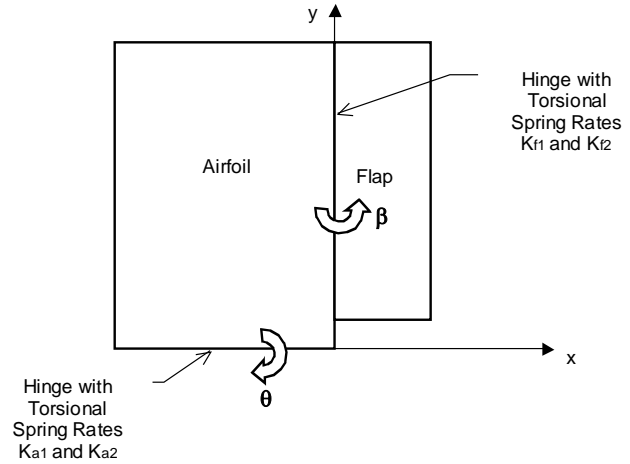


**Figure 4. Model for non-linear flapped VG concept.**

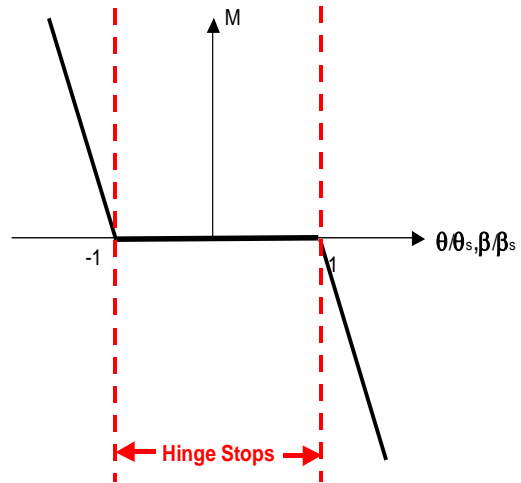


**Figure 5. Spring stiffness as a function of displacement  $x$ .**

thick polypropylene sheet stock using a combination of “living hinges” and hinge stops to provide the non-linear spring rates.

Using the flapped FDOVG simulation model a test configuration was designed which satisfied the target objectives outline above. A dynamic simulation for this configuration with a free stream velocity of 120 ft/s predicted a flap oscillation frequency of 23.4 cycles per second, which corresponds to a wavelength of VG wake oscillation of  $\lambda/c=20.5$  chords. The predicted amplitude of motion of the root hinge is  $\pm 10$  degrees and the flap hinge is  $\pm 30$  degrees.

The flutter onset speed can be predicted using this model by varying the free stream velocity and determining the resulting system response. The onset flutter speed for this configuration is predicted to be  $U_{Flutter}=67$  ft/s. For speeds above 67 ft/s a sustained limit cycle oscillation is obtained. For speeds below 67 ft/s a damped oscillatory response is predicted. Based on the preliminary design sizing study a 3” nominal chord and span test model was fabricated for testing. Figure 6, left, shows the VG test model mounted in the CDI wind tunnel without flow. The “living hinges” and hinge stops were machined to provide spring rates close to those used in simulation. The non-linear springs were incorporated into each hinge through the use of angular stops machined into the mid-section of each hinge. Stops were constructed to allow  $\pm 6$  degrees of motion in the root hinge and  $\pm 25$  degrees of motion for the flap hinge.



**Figure 6. FDOVG wind tunnel demonstration – left: model without flow; right: oscillating VG model operating at  $U=120$  ft/sec.**

The oscillating VG model was found to maintain steady limit cycle flapping motions for tunnel speeds above the flutter onset speed of  $U_{Flutter} = 90$  ft/s (tolerance  $\pm 5\%$ ), which is significantly higher than the predicted flutter onset by the simulation model at 67 ft/s. As noted in Tang, Dowell et al.<sup>10-13</sup>, it is extremely difficult to obtain an accurate prediction of flutter onset speeds and with the level of approximation in this model the predicted and measured flutter onset speeds are judged to be in relatively good agreement. The frequency of oscillation was measured using a strobe light. At 119 ft/s (the maximum attained tunnel speed) the flap frequency of motion was 19 cycles/sec. This frequency corresponds to a wavelength of FDOVG wake oscillation of approximately 20 chords, which is in agreement with that predicted by the simulation model. Figure 6, right, also shows a time-elapsing photo of the oscillating VG flapping motion at this maximum tunnel operating condition. The observed extent of root hinge and flap hinge motions is comparable to those predicted by the model.

These tests clearly demonstrated the feasibility of development of a FDOVG device which can be designed to undergo self-excited limit cycle oscillations at a prescribed amplitude and frequency. Further, with proper design the wavelength of the cyclic vortical structures can be much larger than the VG chord (as with the  $\lambda/c \sim O(20)$  demonstrated here). Finally, the configuration(s) presented here use specially constructed “living hinges” providing both the desired hinge motion and fatigue endurance. However, as will be discussed below, alternate fabrication materials and processes were assessed and successfully implemented as the effort progressed.

### C. Parametric studies of FDOVGs

Using the modeling tools described in the previous section, several arrays of flapped FDOVG devices were designed and fabricated to operate at different LCO frequencies. These initial demonstrator models were constructed ‘by hand’ from steel shim stock of various thicknesses in the 2 to 5 mil range. Figure 7, left, shows a range of the initial prototypes developed in two principal size categories; examination of the figure also reveals details of flap hinge attachments developed for initial examination. Several different FDOVG chord and flap configurations were

also constructed, with designs set so as to initiate oscillation at a range of operating speeds from 30 to 55 fps by balancing size, stiffness, mass, flap hinge overhang, and other parameters. Figure 7, right, shows devices chosen for near full-scale wind tunnel tests based on preliminary calculations and wind tunnel runs at smaller scale. FDOVGs were placed on support pedestals made of flat aluminum plates to minimize interaction of supports with flow and facilitate easy attachment of FDOVGs to wing surface.

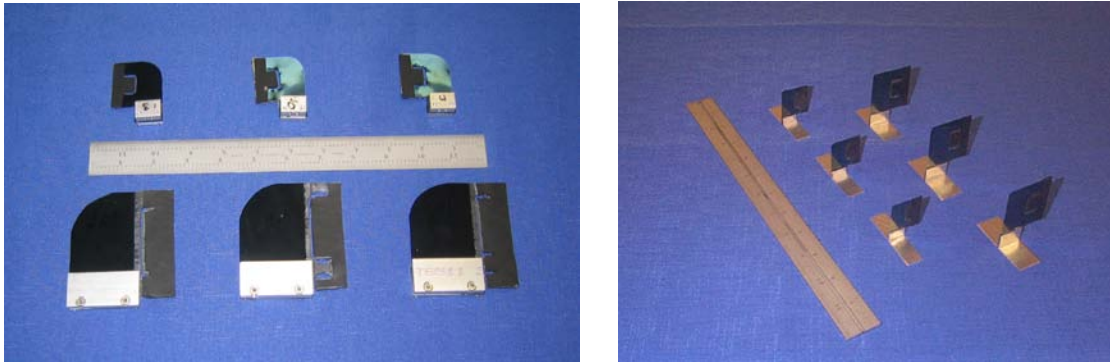


**Figure 7. Several of the initial FDOVG models. Left: small variants (1.5'' by 1.5'' in major dimensions) above, and large variants (3'' by 3'' in major dimensions) below. Right: second-generation FDOVG designs with fixed support pedestals at two different scales – 1.33'' and 2'' high devices.**

To explore the importance of angular orientation it was found expedient to construct several sets of fixed geometry FDOVG devices, identical to the “90 deg.” surfaces shown in Fig. 7, but making a smaller angle with the wing surface. Figure 8 shows these devices (fabricated to produce a 25 degree incidence). Additional sets of devices were built with the same overall dimensions, but at inclinations of 45 deg. to the surface. The intent of these studies was to determine the sensitivity of the effectiveness of the FDOVGs to deployment angle, in order to establish requirements for active devices for deploying FDOVGs selectively.

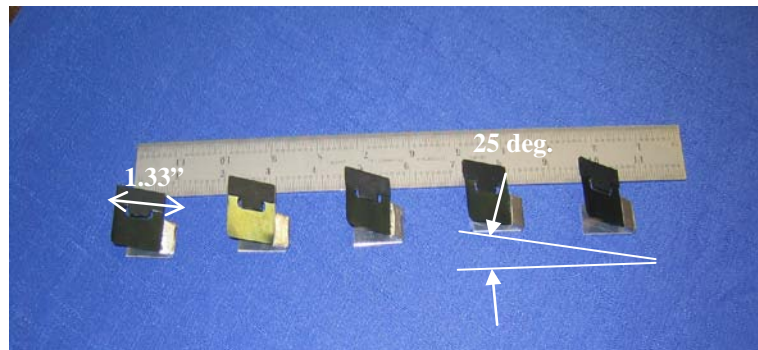


**Figure 8. Fixed 25 degree FDOVG surfaces prior to installation.**

## V. Near Full Scale Wind Tunnel Testing

Arrays of flapped FDOVG devices were used in a series of wind tunnel entries, the first tunnel of which was structured to demonstrate the basic feasibility and effectiveness of the FDOVG concept. Near full scale testing was undertaken in the G.L. Martin Wind Tunnel at the University of Maryland. The array of FDOVGs for this test were mounted on a wing, see Fig. 9, that used a NACA 23015 profile and had a constant chord of 2.0 ft and span of 7.67 ft. The wing was mounted vertically and spanned the full height of the tunnel; angle of attack could be adjusted during the runs and forces and moments on the wing were measured directly from the wind tunnel balance. In this test, side force on the balance equated to lift on the wing, while drag was measured in the conventional downstream direction. The size of the wing and the target flow speeds (50-80 fps) resulted in chord  $Re$  values of of  $0.6-1.0 \times 10^6$ , approaching that of landing configurations for general aviation aircraft.

All the FDOVGs were mounted at zero angle of attack with respect to oncoming flow (i.e., with the chord of the FDOVGs oriented parallel to the wing chord line) and were positioned at the 30% chord location. In the first part of

the experiment, 14 “large” FDOVGs were used (Fig. 7, right, back row); each was of the same size, 2” high by 1.5” long with a 0.75” inch flap. These were tested first with 6” lateral spacing (3.0 device heights) and then an additional 14 FDOVGs were added to provide a 3” lateral spacing (1.5 device heights). Follow-on tests using the small 1.33” by 1” devices (Figure 7, right, front row) were then conducted, first with 3” lateral spacing (2.3 device heights, requiring 28 units) and then with 2” spacing (1.5 device heights, requiring 42 units) (see Fig. 9, right, for the layout of devices in this case).



**Figure 9. Wing mounted vertically in wind tunnel with small FDOVGs installed on the suction surface; array of flow visualization tufts also shown. Left: lateral spacing = 2.3 device heights. Right: lateral spacing = 1.5 device heights.**

Initial testing took place using the larger variant of FDOVGs with tests conducted at flow speeds near the nominal activation speeds of 50-80 fps. All of the tests consisted of angle of attack sweeps for the wing, with angle of attack (AOA) ranging from -5 to 20 deg. An attempt was made to select a tunnel speed which caused the FDOVGs to commence oscillations in the 5-10 deg. AOA range. This typically meant that the devices experienced gradually amplifying oscillations as angle of attack (and effective flow speed over the suction surface of the wing) increased, with an effective “shut off” of oscillations once the stall angle of attack was passed. As will be seen, the cases examined here resulted in significant increases in stall angle of attack and maximum lift coefficient.

For the large (2”) FDOVGs, the selected tunnel speed was 50 fps; preliminary runs at 45 and 55 fps indicated that the former developed relatively weak oscillations, while the latter produced very energetic oscillations that led

to damage to two devices. Figure 10 summarizes the lift coefficient results for the large FDOVG case; here it is evident that the devices produced very significant favorable results, increasing stall angle of attack by roughly 2.5 deg. for a spacing of 3.0h (14 FDOVGs along the span) and by 5 deg. for a spacing of 1.5h (28 FDOVGs on the span). Though not shown on this plot, observations during the test indicated stall occurred just beyond 20 deg. AOA for the latter case. For these two cases, the maximum  $C_L$  achieved is 1.48 and 1.70, respectively, as compared to the baseline maximum  $C_L$  of 1.22. The latter case corresponds to a 40% increase in maximum  $C_L$ .

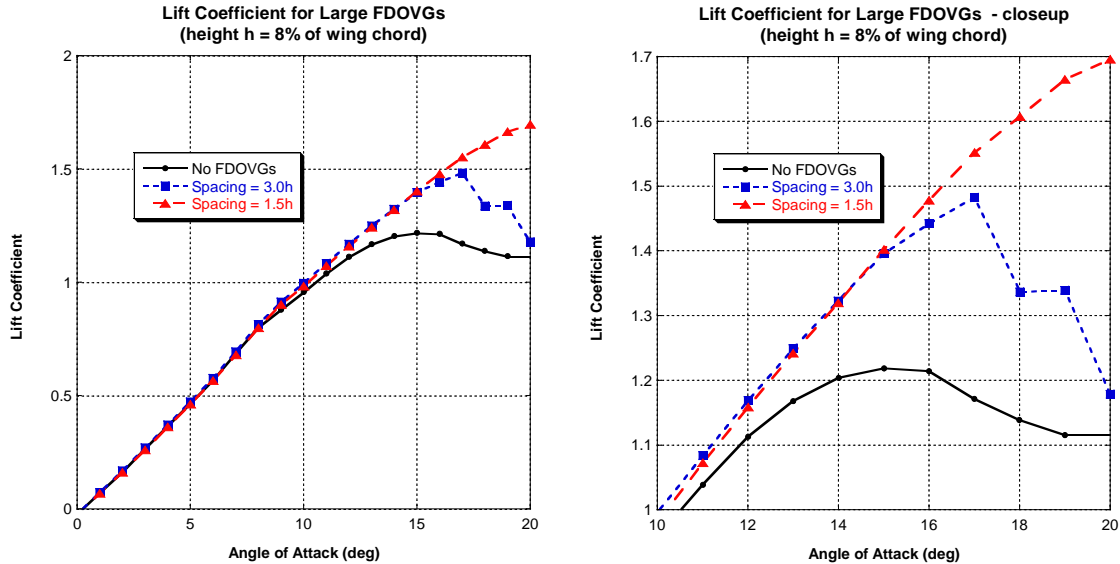
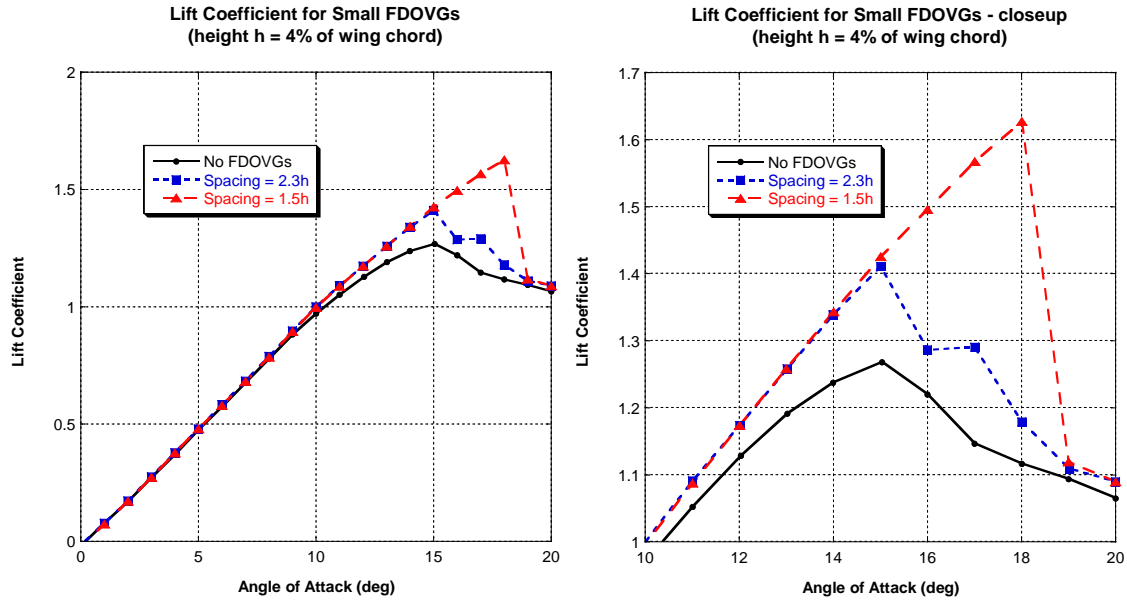


**Figure 10. Lift coefficient results for large FDOVGs; closeup of high lift region at right.**

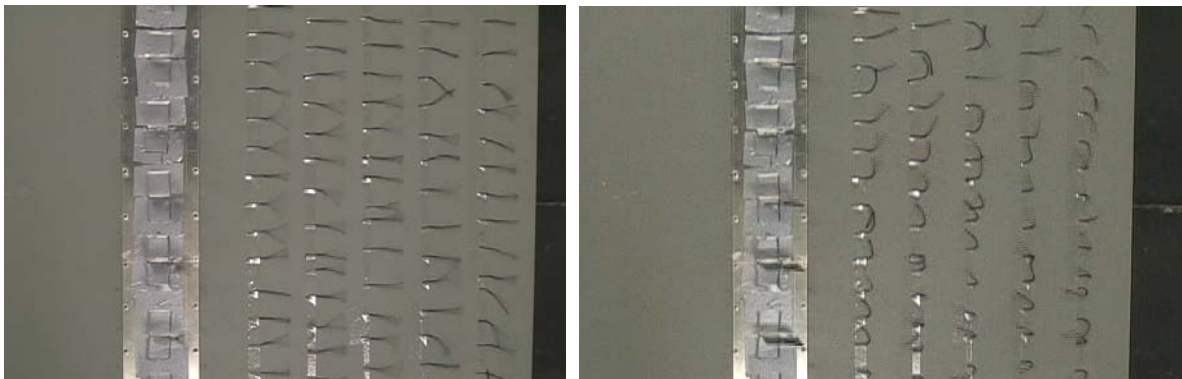
Moving to the case of the small (1.33") FDOVGs, for this case a tunnel speed of 85 fps was selected. Figure 11 summarizes the lift coefficient results for this case, which are qualitatively similar to those for the larger FDOVGs and, though smaller in magnitude, remain very significant. The increase in stall angle of attack is only roughly 0.5 deg. for a device spacing of 2.3h, though it increases by fully 3 deg for a 1.5h spacing; the corresponding maximum lift coefficients are 1.41 and 1.63, which offer large increases in lift compared to the baseline  $C_L$  of 1.27. Thus, even these smaller devices offer up to a 28% increase in maximum lift coefficient.

Figure 12 shows snapshots of tuft visualization results that correspond to these cases; these pictures indicate the ability of the FDOVGs to promote flow attachment. The visual history of the tuft array also reflects the abrupt drop in lift evident in the figures above; when angle of attack increases sufficiently to cause the FDOVGs to stop, the lift returns to the level observed for the unmodified wing.

Further insight into the effect of these devices on wing performance is given in Figure 13, which shows the effect of the various options on drag. Comparison of the plots in Fig. 13 shows that the large FDOVGs produce a significantly greater drag increment than small FDOVGs. An equally interesting observation is to compare the lift/drag polar of a case with small FDOVGs to one with a typical flap arrangement for high lift, e.g., a full-span 20% chord plain flap. Using semi-empirical characteristics from standard aeronautical design guides, an approximate polar can be constructed for a flapped NACA 23015 that produces the same increase in maximum lift coefficient as was achieved with the small FDOVGs. Figure 14 shows the comparison of this case with the others discussed above; as is evident, even for this highly non-optimized early design of the FDOVGs, the drag at maximum lift for the 1.5h spacing case is close to that estimated for the plain flap. Thus, a more optimized case could be competitive with or even superior to conventional flapped wings in providing a good lift/drag tradeoff; this raises the possibility leveraging the capability of FDOVGs to permit a wing to be built with the flap system removed or reduced in size.



**Figure 11. Lift coefficient results for small FDOVGs; closeup of the high lift region at right.**



**Figure 12. Tuft flow visualization for the large FDOVGs. 1.5” device height spacing; attachment maintained up to and past 18 deg. angle of attack, left; with flow separation at 20 deg., right.**

Following these tests, additional experiments were conducted using the devices with 25 and 45 deg, inclination to the surfaces (Fig. 15). The first studies conducted involved angle of attack sweeps at a constant tunnel speed of 85 fps; this speed was selected so that the FDOVGs were fully engaged in LCO motion by the point at which an angle of attack of 10 deg. was reached. The addition of the FDOVGs adds a very large increment in maximum lift (a 29% increase to a  $C_L$  of 1.65 for the 90 deg. case). The increment is smaller but still very substantial for the 45 deg. case (19% increase in maximum  $C_L$ ); interestingly, the 25 deg. case yields an improvement in maximum lift behavior relative to the 45 deg. case, i.e., a 24% increase in maximum lift over the “clean wing” case. A possible inference from this is that there is some benefit to use of low-inclination FDOVG surfaces, in that they contribute both spanwise and streamwise components of vorticity to the downstream flow field.

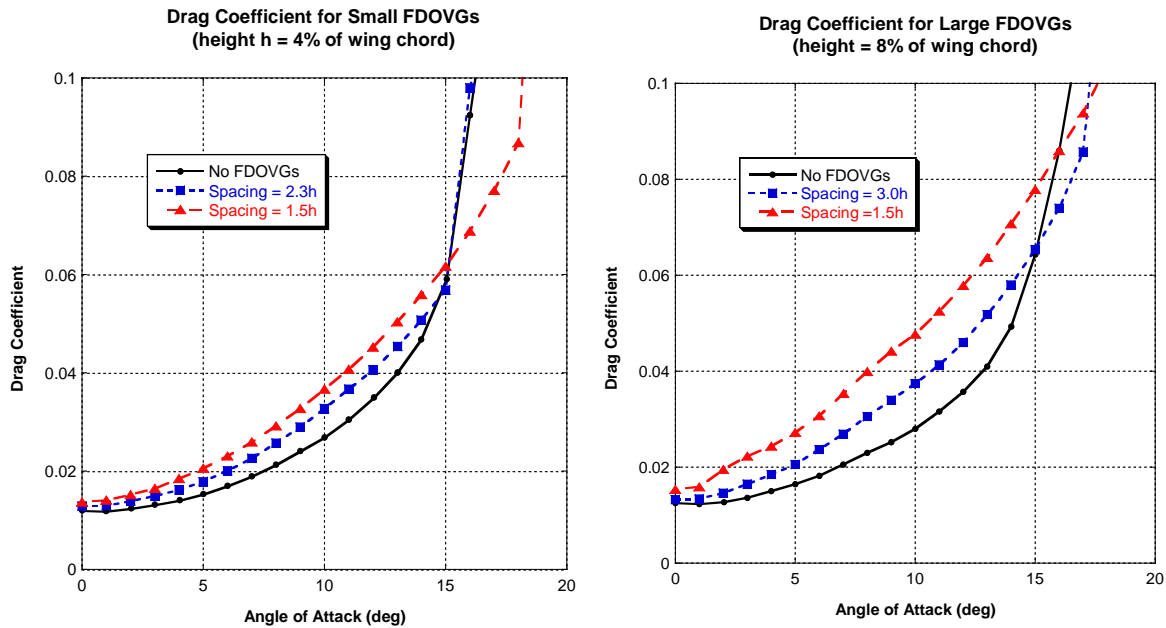


**Figure 13.** Summary of drag polars for the two different classes of FDOVGs; small FDOVGs at left, large devices at right.

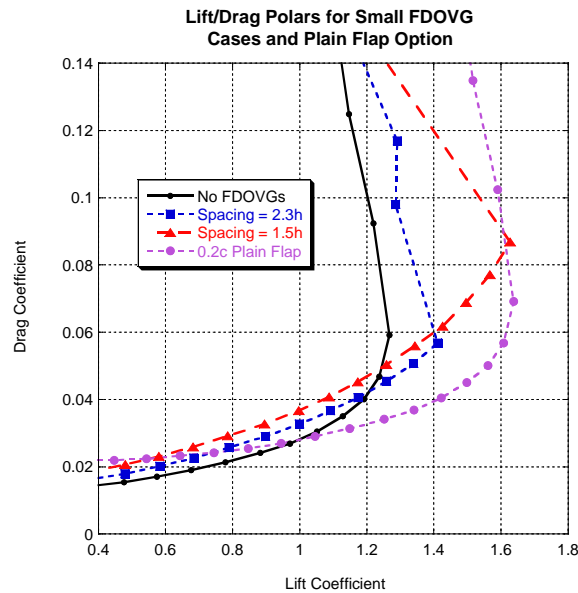


**Figure 14.** Comparison of lift/drag polars for small FDOVG case compared to 20% chord plain flap providing the same maximum lift coefficient.

Examining the lift to drag ratio (Fig. 16) yields additional results, notably that above 14 deg. angle of attack, all FDOVG options offer a better L/D than the baseline wing. In the critical region approaching stall, the 25 deg. inclination devices yield results almost as favorable as the 90 deg. devices. The importance of this point is that adoption of a lower inclination angle could greatly reduce the design challenge of building deployable FDOVGs in that deployment to 25 deg. inclination to the surface is much more readily accomplished than deployment to a full 90 deg.

An additional aspect of interest for these devices is addressed in Fig. 17, which presents results from wing angle of attack sweeps for a case using the 25 deg. inclination FDOVGs. Two runs are compared, the first with a free stream speed of 60 fps (below the activation speed of the oscillating VGs) and second at a free stream speed of 85 fps (with FDOVGs operating). Comparing the results of these two cases, it is evident that while the presence of the OVG surfaces themselves contributes to an enhancement in maximum lift coefficient (from a peak of 1.24 to 1.30) the effect of the oscillating VGs is by far the major contributor, permitting a peak lift coefficient of 1.60. This comparison clearly demonstrates that it is the unsteady, self-excited oscillations of the FDOVGs – rather than the effect of their mean position – that produces the primary effect in enhancing peak lift levels.

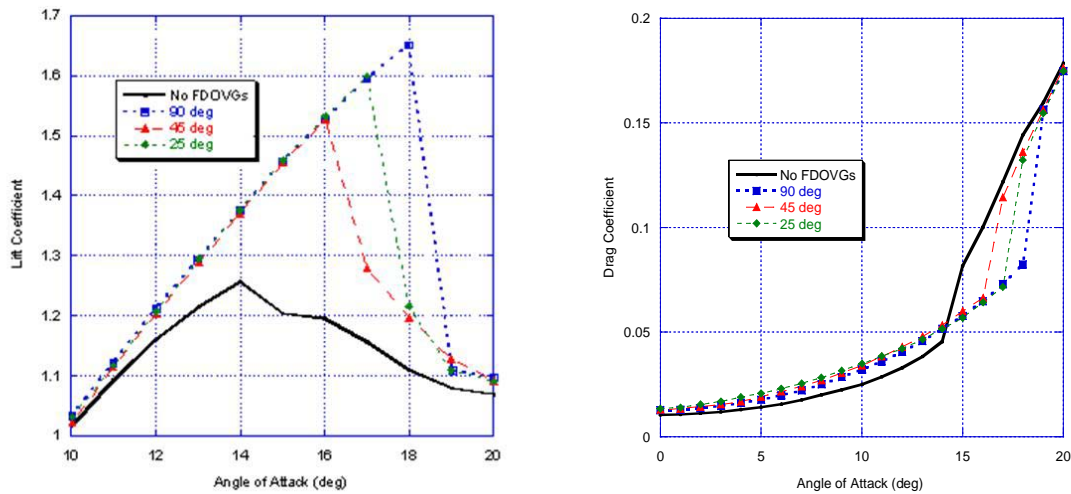


Figure 15. Comparison of lift coefficient (left) and drag coefficient (right) for angle of attack sweeps using the FDOVGs with reduced angular inclination; comparisons shown with the 90 deg. inclination cases as well as with the baseline wing.

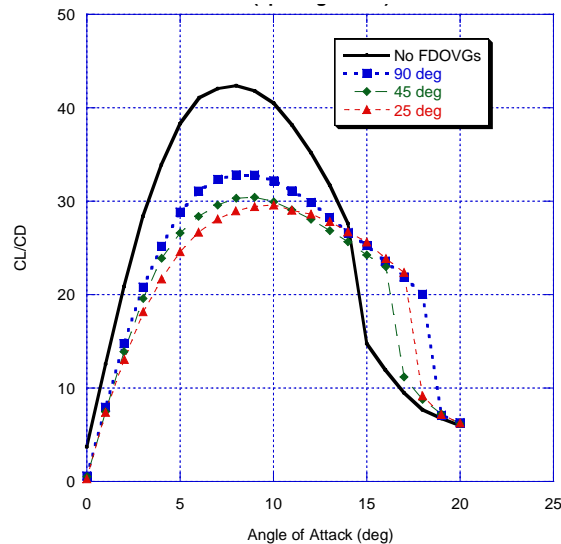
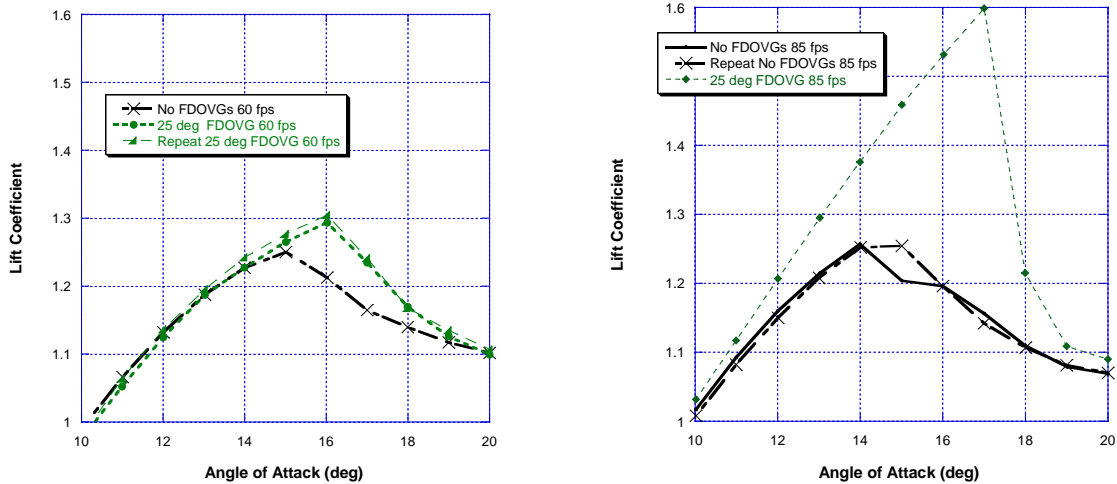


Figure 16. Lift to drag ratio for angle of attack sweeps using the FDOVGs with reduced angular inclination; comparisons shown with the 90 deg. inclination cases as well as with the baseline wing.



**Figure 17. Lift coefficient for angle of attack sweeps using the FDOVGs with 25 deg. angular inclination; comparisons shown between cases with free stream velocity below (left) and above (right) FDOVG activation speed.**

## VI. Conclusion

Flow Driven Oscillating Vortex Generators (FDOVGs) are an innovative mechanical mechanism to introduce cyclic vortical structures into boundary layers to delay or prevent flow separation, with the potential for extension to applications such as stabilizing free shear layers. FDOVGs take advantage of aeroelastically designed limit cycle oscillatory (LCO) motions, using the energy extracted from the free stream to drive the oscillatory motion. The FDOVG has many potential advantages over other active control technologies in terms of the ease with which it can be transitioned to a wide range of aircraft, marine and ground vehicle applications. First, since it is self-excited it does not require an actuation mechanism to produce a flow control effect, though active deployment may be desirable. Second, it can be surface mounted with minimal penetration of the body, making retrofit an option in addition to its suitability for incorporation into new aircraft configurations. Third, as was anticipated based prior active control research, the cyclic vortical structures introduced by the FDOVG can substantially enhance momentum transfer and mixing within the boundary layers for increased separation control. Based on preliminary concept development, it was expected that any penalty for removing this energy from the free stream when the FDOVG is oscillating will be more than compensated by the performance gain from the boundary layer control.

A natural focus for follow-on work will be the assessment of candidate deployment devices, e.g., where the FDOVG stows flush with the mold line when not in use, as well as “Oscillation on Demand” implementations - where the FDOVG stays positioned in the flowstream, switching between self-excited and non-excited as a result of changes in flow conditions or through positive actuation. Additional possible future research efforts include: a flight test in which an array of FDOVGs on would be mounted on general aviation aircraft or unmanned air vehicle to demonstrate potential for enhancing aircraft performance and mitigating flow separation; a test of an array of FDOVGs on a full-scale tractor-trailer as part of initiative to reduce fuel consumption and costs in the trucking industry; and possible testing of modified FDOVGs for military applications such as stabilizing shear layers and mitigating cavity flow oscillations in weapons bays.

## Acknowledgements

This research was supported by NASA/Langley Research Center under contract NAS1-02160. The technical monitor was Dr. J.C. Lin. The authors also wish to acknowledge technical support on OVG design from Drs. A.J. Bilanin and W.J. Usab, Jr. as well as the support of Mr. R.S. Snedeker in construction of the wind tunnel model.

## References

1. Taylor, H.D., "The Elimination of Diffuser Separation by Vortex Generators," Report, United Aircraft Corporation, June 1947.
2. Lin, J.C., "Control of Turbulent Boundary-Layer Separation Using Micro-Vortex Generators," AIAA-99-3404, June 1999.
3. Seifert, A., Darabi, A., and Wynanski, I., "Delay of Airfoil Stall by Periodic Excitation," Journal of Aircraft, Vol. 33, No. 4, pp. 691-698, July-August 1996.
4. Seifert, A. and Pack, L.G., "Oscillatory Control of Separation at High Reynolds Numbers," AIAA Journal, Vol. 37, No. 9, pp. 1062-1071, September 1999.
5. McManus, K.R., Legner, H.H., and Davis, S.J., "Pulsed Vortex Generator Jets for Active Control of Flow Separation," AIAA 94-2218, 25th AIAA Fluid Dynamics Conference, Colorado Springs, CO, June 20-23, 1994.
6. Gallas Q., Wang G., Papila M., Sheplak M., Cattafesta L., "Optimization of Synthetic Jets Actuators", AIAA 2003-0635, 41<sup>st</sup> Aerospace Sciences Meeting & Exhibit, Reno, NV, January 6-9, 2003
7. Wiltse, J.M. and Glezer, A., "Manipulation of Free Shear Flows Using Piezoelectric Actuators," Journal of Fluid Mechanics, V. 249, pp. 261-285, 1993.
8. Qayoum A., Gupta V. and Panigrahi P., "Turbulent Boundary Layer Manipulation using Synthetic Jet Actuation", Proc. of the World Congress in Engineering (WCE), Vol. II, July 1-3, 2009, London, U.K.
9. Seifert A., "Closed-Loop Active Flow Control Systems: Actuators", in "Active Flow Control", "Notes on Numerical Fluid Mechanics and Multidisciplinary Design", Vol. 95, pp. 85-102, 2007.
10. Tang, D., Dowell, E.H., and Hall, K.C., "Limit Cycle Oscillations of a Cantilevered Wing in Low Subsonic Flow," AIAA Journal, Vol. 37, No. 3, pp. 364-371, March 1999.
11. Tang, D., Henry, J.K., and Dowell, E.H., "Limit Cycle Oscillations of Delta Wing Models in Low Subsonic Flow," AIAA Journal, Vol. 37, No. 11, pp. 1355-1362, November 1999.
12. Dowell, E., Hall, K.C., Thomas, J.P., et al., "Reduced Order Models in Unsteady Aerodynamics," Engineering Mechanics, Vol. 6, No. 4/5, pp. 229-252, 1999.
13. Tang, D.M., Virgin, L., and Dowell, E., "Limit Cycle Behavior of an Airfoil with a Control Surface," Journal of Fluids and Structures, Vol. 12, No. 7, December 1998.